




Superhydrophobic and magnetic PS/Fe₃O₄ sponge for remote oil removal under magnetic driven, continuous oil collection, and oil/water emulsion separation

Haoran Huang¹, Xin Li¹, Chunxia Zhao^{1,*} , Longbin Zhu¹, Yuntao Li^{1,*}, Yuanpeng Wu¹, and Zhenyu Li¹

¹ College of New Energy and Materials, Southwest Petroleum University, Chengdu 610500, China

Received: 2 May 2021

Accepted: 25 September 2021

Published online:
3 January 2022

© The Author(s), under exclusive licence to Springer Science+Business Media, LLC, part of Springer Nature 2021

ABSTRACT

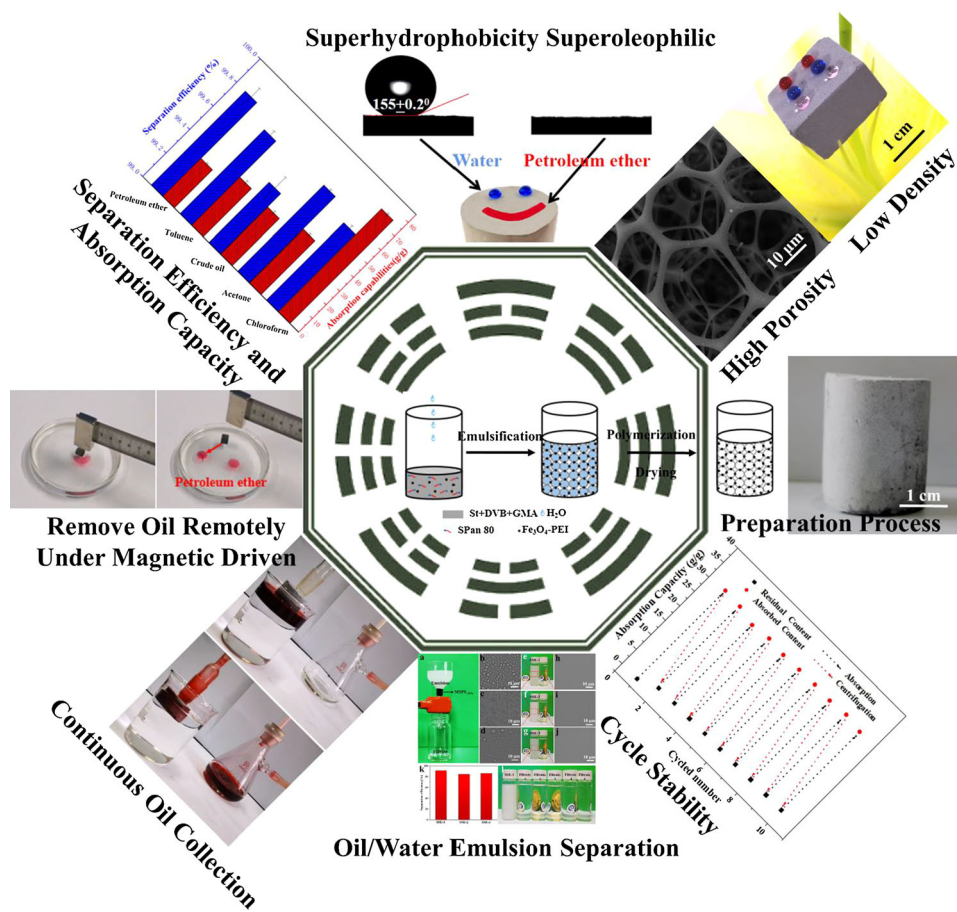
Superhydrophobic and magnetic materials with multiple functions (e.g., continuous oil collection, remote oil removal in confined spaces under magnetic driven, separation of oil/water emulsions, and good oil absorption capacity with robust stability) are highly required for practical oily wastewater remediation, but still a challenge to be realized. For this purpose, superhydrophobic Fe₃O₄ nanoparticles/polystyrene (PS) composite sponge has been fabricated via high internal phase emulsion template method. The as-prepared sponge exhibits high water-repellence and superoleophilicity with water/oil contact angles are 155° and 0°, respectively. Given the magnetic properties of Fe₃O₄, our sponge displays the capacity for remote oil capture under magnetic driven. Additionally, continuous oil collection has been also realized with the equipment of pumper. Different from some previous reported sponges, our sponge also possesses the unique ability to separate surfactant stabilized oil/water emulsion. Besides, our sponge can also act as a high-efficiency oil absorbent with robust cycling stability (oil recovery rate can reach 92%, even after 10 absorption-centrifugation cycles). These outstanding functions make our sponge hold great potential for the purification of oily wastewater.

Handling Editor: Dale Huber.

Address correspondence to E-mail: polychem2011@hotmail.com; yuntaoli@swpu.edu.cn

GRAPHICAL ABSTRACT

This work reported a simple and environmentally-friendly approach to prepare multi-functional magnetic and superhydrophobic sponges via high internal phase emulsion (HIPE) method. The PS/Fe₃O₄ composite sponges exhibited unique properties: (i) high water-repellence and good oleophilicity; (ii) the function as a high-efficiency oil absorbent with robust cycling stability; (iii) ability to remove oil remotely under magnetic driven; (iv) continuous oil collection; (v) the capacity to separate surfactant stabilized oil/water emulsion. These outstanding performances make our sponge is of great importance for practical oily wastewater remediation.



Introduction

Frequent oil spills and the discharge of large amounts of industrial oily wastewater have caused serious environmental pollution and huge economic losses all over the world [1]–[3]. Traditional methods for

oily wastewater purification (e.g., chemical reagent dispersal [4], centrifugation [5], *in-situ* incineration [6], skimmer collection) [7], usually face some problems such as high energy consume, low separation efficiencies, and secondary pollution. Recently, superhydrophobic materials-based bionic strategies have gained special attentions for their unique

capacity to selectively remove oil from wastewater [8]–[18]. Su et al. used F-Fe₃O₄ nanoparticles and PDMS under a static magnetic field to adjust the surface morphology and wetting method by changing the ratio of F-Fe₃O₄ nanoparticles to PDMS. Utilizing the asymmetric adhesion properties of superhydrophobic fabrics, it has been successfully applied to lossless droplet transmission and oil/water separation [8]. Li et al. used trimethylsilyl-terminated-poly-(dimethylsiloxane)-co-polymethylhydrosiloxane (PDMS-co-PMHS) to coat the surface of the sponge skeleton and successfully applied the modified sponge to oil/water separation [19]. Zhou et al. have prepared superhydrophobic RGO@PU sponges via dip-coating and solvothermal treatment with the assistance of ethanol, which can be applied to separate oil/water mixtures [20]. Among diverse superhydrophobic materials, superhydrophobic sponges (SSs) are of particular interest due to their high oil removal/absorption properties [21]–[24]; however, most reported SSs can only remove/absorb oil on the top of aquatic systems, which could not be applied in collecting oil under water or at some confined locations.

To enhance the oil capture capacity of these SSs, decoration of magnetic materials with SSs have been widely investigated owing to these composite sponges can remotely capture oil under magnetic driven [25]–[31]. For example, Wang et al. prepared magnetic superhydrophobic sponges by simply modifying commercial sponges with PDA/Fe₃O₄ nanoparticles and then used them to remove underwater oil via a remotely controlled external magnetic field [32]. Boukherroub et al. modified polyurethane sponge with Fe₃O₄ and high-density polyethylene and used it to separate an oil and water mixture, as well as demulsification [33]. Zhan et al. designed a new type of magnetically driven three-dimensional superhydrophobic carbon fiber material for continuous oil/water separation in harsh environments [34]. Shi et al. prepared a magnetic superhydrophobic porous materials through Fe₃O₄ nanoparticles, dopamine and fluorine-containing siloxane modified polyurethane sponge [35]. Although many successes have been achieved, constructing magnetic SSs with continuous oil collection, remote oil removal in confined spaces under magnetic driven, separation of oil/water emulsions, and good oil absorption capacity with robust stability, is still a challenging to be realized.

Herein, we report a simple and environmentally friendly approach to prepare aforementioned multifunctional magnetic and superhydrophobic sponge via high internal phase emulsion (HIPE) method, in which Fe₃O₄ nanoparticles were decorated with polystyrene (PS) sponge. The addition of Fe₃O₄ nanoparticles not only imparted a magnetic response to the material, but also beneficial for enhanced hydrophobicity (water contact angle is as high as 155°) for the formation of hierarchical micro-nanostructures on the surface of PS sponges. Our Fe₃O₄/PS composite sponge exhibited some unique properties: (i) high water-repellence and good oleophilicity (water/oil contact angles are 155° and 0°, respectively); (ii) the function as a high-efficiency oil absorbent with robust cycling stability; (iii) ability to remove oil remotely under magnetic driven; (iv) continuous oil collection; (v) the capacity to separate surfactant stabilized oil/water emulsion; these outstanding performances make our sponge is of great importance for practical oily wastewater remediation.

Materials and methods

Materials and reagents

Styrene (St), divinylbenzene (DVB), glycidylmethacrylate (GMA), Span80, azobisisobutyronitrile (AIBN), iron(III) chloride hexahydrate (FeCl₃•6H₂O), sodium acetate (NaAc), toluene, ethylene glycol (EG), and absolute ethanol were all purchased from Chengdu Kelong Chemical Reagent Factory. Polyethyleneimine (PEI, branched, *M_w* = 70,000, 50% aqueous solution) was purchased from Innochem Technology Co., Ltd., Beijing. Deionized water was used throughout the experiments. All chemicals were of reagent grade and used without further purification.

Synthesis of amine-functionalized Fe₃O₄ nanoparticles (Fe₃O₄-PEI)

Amine-functionalized Fe₃O₄ nanoparticles were synthesized by a solvothermal method [36]. In a typical approach, FeCl₃•6H₂O (13.5 g) was first dissolved in 150 mL EG by mechanical stirring to form a transparent solution. Then, NaAc (12.0 g) was added to the FeCl₃ solution to form uniformly dispersed solution. Finally, PEI (6.0 g) was added in and stirred

vigorously until dissolved. The above mixture was stirred vigorously at room temperature for 0.5 h and then transferred to a Teflon-lined stainless steel autoclave and reacted at 200 °C for 8 h. The black product ($\text{Fe}_3\text{O}_4\text{-PEI}$) was washed with deionized water and absolute ethanol and collected by an external magnetic field.

Preparation and polymerization of high internal phase emulsions (HIPE)

During the HIPE synthesis, Span 80 (0.15 g), AIBN (0.05 g) initiator, and $\text{Fe}_3\text{O}_4\text{-PEI}$ nanoparticles (0.05 g) were ultrasonically dispersed in an oil phase consisting of St (0.15 g), GMA (0.1 g), and DVB (0.25 g). Deionized water was gradually added to the above mixture. After adding 2 mL of water each time, the system was vigorously shaken by hand until a sticky and uniform HIPE was formed. The as-prepared HIPE was put in a convection oven, and the organic monomers were polymerized at 65 °C for 8 h. The obtained grey monolith was soaked in absolute ethanol to remove residual surfactant and monomers and then dried in a convection oven at 50 °C for 10 h. Finally, a magnetic superhydrophobic polystyrene-based porous material containing 10 wt% $\text{Fe}_3\text{O}_4\text{-PEI}$ was obtained and labeled as $\text{MSPS}_{-10\%}$. The samples of $\text{MSPS}_{-5\%}$, and $\text{MSPS}_{-15\%}$ were prepared via the same route. The monolith prepared without $\text{Fe}_3\text{O}_4\text{-PEI}$ nanoparticles was labeled as a hydrophobic polystyrene-based porous material (HPS). The

production process of the hierarchical skeleton is schematically illustrated in Scheme 1.

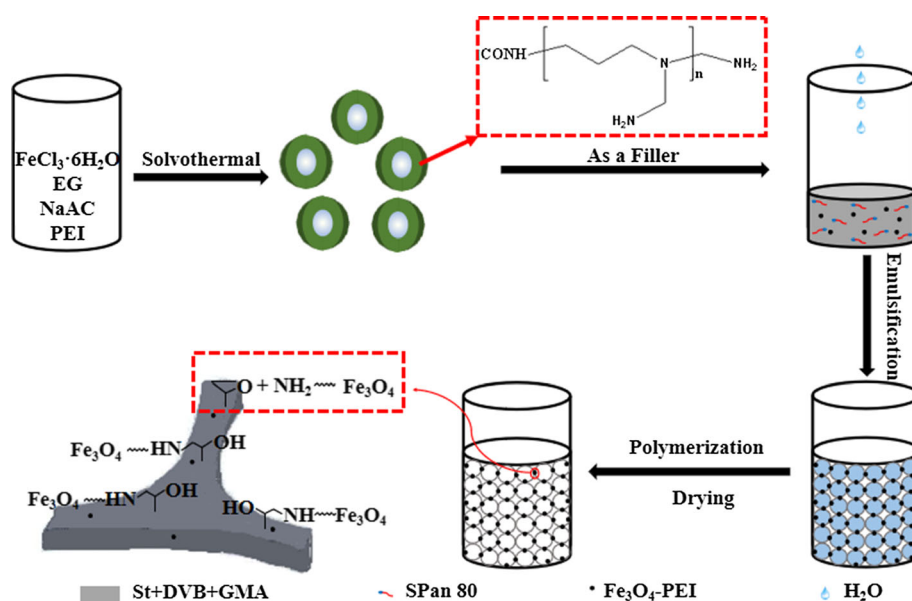
Characterization

The surface morphology of $\text{Fe}_3\text{O}_4\text{-PEI}$ nanoparticles and the monolith were characterized by scanning electron microscopy (SEM, JEOL JSM-5009LV) at an accelerating voltage of 20.0 kV. The elemental composition of samples was characterized by energy-dispersive spectroscopy (EDS) accompanied by SEM. Transmission electron microscopy (TEM) images were obtained by a JEOL JEM-2100 F transmission electron microscope (JEOL, Tokyo, Japan). Fourier-transform infrared spectroscopy (FTIR, Nicolet 6700, Thermo Fisher Scientific, USA) was used to determine the chemical composition of the materials, and the absorption spectra were recorded from 500 cm^{-1} to 4000 cm^{-1} . X-ray diffraction (XRD) analysis was performed using a DX-2700 diffractometer with $\text{Cu K}\alpha$ radiation. An automatic mercury porosimeter (AutoPore IV 9500) was used to test the density, porosity and pore size distribution of porous materials. Karl Fischer moisture tester (Mettler V10S) was utilized to test the water content in the liquid before and after the separation of the oil/water emulsion.

Surface wettability measurements

Water contact angles (WCA) and oil contact angles (OCA) of the monolith surface in the air were measured using a contact angle goniometer (OCA 25,

Scheme 1 Schematic illustration of the fabrication of the superhydrophobic and magnetic PS/ Fe_3O_4 sponge.



Data physics Instruments GmbH, Germany) using 3 μL deionized and petroleum ether droplets at five different locations on each sample.

Ability to remove oil remotely under magnetic driven

To broaden the range of superhydrophobic sponge, Fe_3O_4 -PEI nanoparticles were decorated with polystyrene sponge. The MSPS-10% can be pushed and accurately guided by magnetic force to follow a predetermined path to the contaminated site.

Continuous oil collection tests

For continuous collection of floating oil in situ from seawater, a simple oil collection apparatus was utilized to measure the oil/water separation ability of MSPS-10% at the dynamic state during pumping.

The saturated oil absorption capacity

To investigate the saturated oil absorption capacity of the materials, a variety of organic solvents and oils were used, and the results can be described by formula 1:

$$A_C = \frac{M_a - M_b}{M_b}$$

where A_C (g/g) is the saturated oil absorption capacity of the material, and M_a and M_b are the mass of the materials after and before reaching saturated oil absorption, respectively.

The oil/water mixture separation efficiency

The oil/water mixture separation efficiency was calculated using this formula 2 [19]:

$$v = \frac{m_a}{m_b} \times 100\%$$

Herein, m_b and m_a were the mass of water before and after separation, respectively.

Separation of surfactant-stabilized emulsions

To simulate the real stable emulsions in practical application, three kinds of surfactant-stabilized water-in-oil (W/O) emulsions were prepared. The

water-in-petroleum ether emulsion was marked as SSE-1, SSE-2 for the water-in-toluene emulsion and SSE-3 for the water-in-chloroform emulsion, respectively, the mentioned emulsions were prepared by mixing oil and water ($V_{\text{oil}}: V_{\text{water}} = 99:1$) with 5 g/L Span 80 surfactant and stirring for 3 h.

The separation efficiency (E) of the emulsion can be determined by calculations using the following formula 3 [37]:

$$E = (1 - \frac{C_s}{C_0}) \times 100\%$$

Herein, C_0 and C_s refer to the water content in the original W/O emulsion and the separated liquid, respectively. Water content in the separated filtrate was analyzed by the Karl Fischer analyzer.

Results and discussion

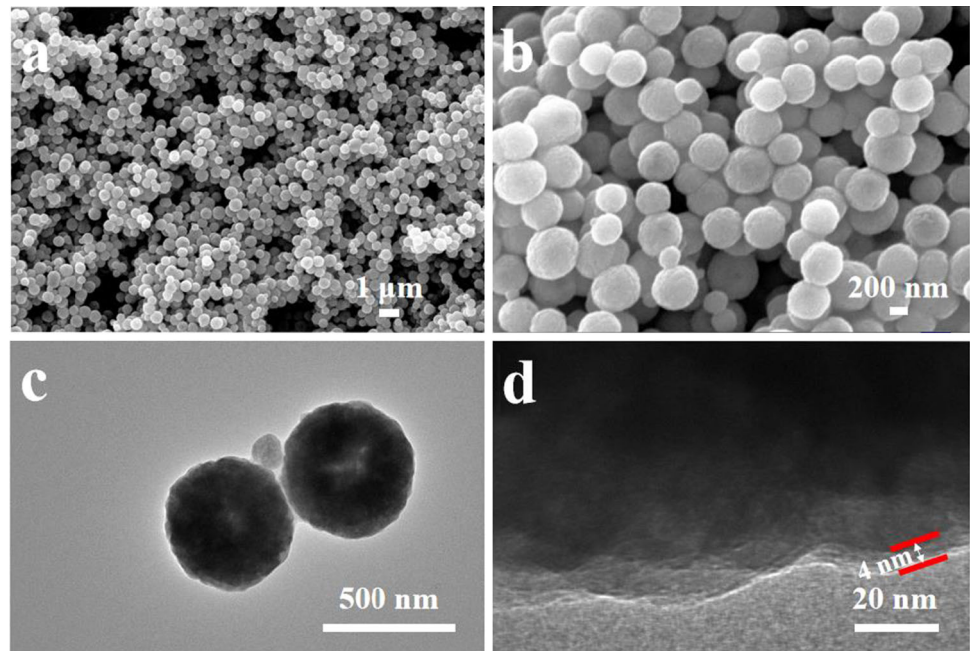
The morphology of the Fe_3O_4 -PEI particles

SEM has been used to characterize the as-prepared Fe_3O_4 -PEI nanoparticles as shown in Fig. 1a, b with low and high magnifications, respectively, indicating the spherical shape of the nanoparticles and the average diameter is about 350 ± 20 nm. The crystal structure of Fe_3O_4 -PEI nanoparticles has been characterized by XRD (ESI; Fig. S1). Five typical diffraction peaks of (220), (311), (400), (511), and (440) planes towards cubic Fe_3O_4 -PEI crystal structure have been observed [38]. To confirm the existence of PEI, EDS and FTIR have been combined to characterize the Fe_3O_4 -PEI nanoparticles (ESI; Fig. S2 and Fig. S3). The N elements from PEI could be detected clearly by EDS. For the FTIR spectrum, the peak at 582 cm^{-1} is ascribed to the stretching vibration of Fe–O–Fe. The peaks at 1042 ($\delta_{\text{C-N}}$) and 1632 cm^{-1} ($\delta_{\text{N-H}}$), 2920 and 2961 cm^{-1} are according to the asymmetric and symmetric stretching vibrations of $-\text{CH}_2-$ in PEI [36, 39], respectively. Figure 1c, d display the TEM images of the as-prepared Fe_3O_4 -PEI nanoparticles, confirming the thickness of PEI coating layer is about 4 nm. EDS, FTIR and TEM confirm the existence of PEI on the outer surface of Fe_3O_4 nanoparticles.

Morphologies of Fe_3O_4 /PS composited sponges

SEM has been used to characterize the morphologies of Fe_3O_4 /PS composited sponges with various Fe_3O_4 -PEI nanoparticles loading as shown in Fig. 2. As for

Figure 1 SEM images (a and b) and TEM images (c and d) of Fe₃O₄-PEI nanoparticles.



pristine PS sponge, high porosity with three-dimensional interconnected network structure could be observed (Fig. 2a1–a3). The pore size of PS sponge was about $25 \pm 3 \mu\text{m}$. As the loading content of Fe₃O₄-PEI nanoparticles was 5 wt%, the porosity was not changed (Fig. 2b1, b2). Fe₃O₄-PEI nanoparticles could be detected on the outer surface of PS sponge (Fig. 3b), forming the hierarchical structures on the outer surface and benefiting for enhanced superhydrophobicity. Further enhance the loading content to 10 wt%, more Fe₃O₄-PEI nanoparticles could be detected on the outer surface of sponge (Fig. 2c1–c3). As the loading content was as high as 15 wt%, some of pores, formed in the skeleton, could be detected for the serious agglomeration of Fe₃O₄-PEI nanoparticles (Fig. 2d1–d3) [40, 41], which deteriorated the performances of composite sponge. The continuity of molecular chain was broken by excessive solid nanoparticles, without polymerization of monomer molecules around nanoparticles, thus forming windows in the skeleton [42]. The test of pore size distribution through the automatic mercury porosimeter and the result is shown in Fig. S4. With the content increase of Fe₃O₄ nanoparticles, the pore size distribution becomes narrower. Nanoparticles promote the stability of the system, thereby reducing the merging of small droplets into one large droplet [41, 43]. Thanks to the combined structure of large pores and small pores, the large pores can realize the rapid

absorption oil through capillary force, and the small pores can realize the separation of oil/water emulsion through the “size screening effect” [37, 44]. Therefore, the as-prepared sponges are expected to be used for the separation of oil/water emulsions. In addition, as the increasing of Fe₃O₄ nanoparticles content, the density gradually increases but the porosity is similar (ESI; Table S1). It was found that the experimental density was higher than the theoretical value and the experimental porosity was lower than the theoretical value, may be due to the presence of closed cells inside the sample [31].

The decoration of Fe₃O₄-PEI nanoparticles throughout the PS sponge could be attributed to the strong interactions between PEI and PS as proven by FTIR spectrum (ESI; Fig. S3). The weakened absorption peak at 839 and 907 cm^{-1} , in the meantime the enhanced absorption peak at 3435 cm^{-1} , confirmed the reaction of the primary amine of Fe₃O₄-PEI with the epoxy group on GMA via a ring-opening reaction [45]. Upon increasing the nanoparticle content, the water contact angle gradually increased. The water contact angle (WCA) of HPS was only 145.5°, but the WCA of MSPS_{-10%} reached 155°. Increasing the nanoparticle content further increase the roughness, which increased the water contact angle. Upon further increasing the Fe₃O₄-PEI nanoparticles content, the degree of agglomeration of nanoparticles increased, which was unfavorable for the

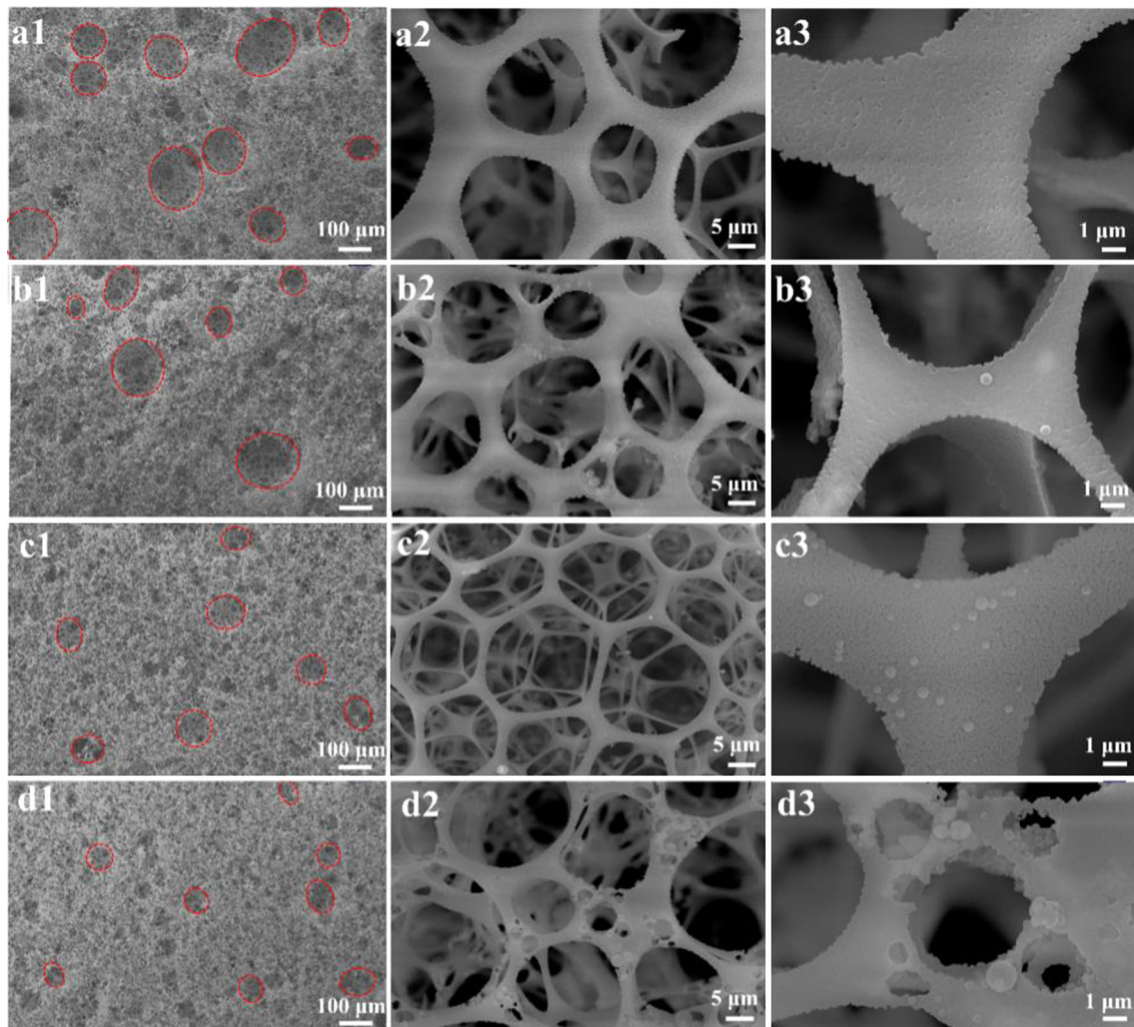


Figure 2 SEM images of (a1, a2 and a3) HPS, (b1, b2 and b3) MSPS-5%, (c1, c2 and c3) MSPS-10%, and (d1, d2 and d3) MSPS-15%.

construction of micro-nanostructures, which decreased the water contact angle (ESI; Fig. S5). Thus, $\text{Fe}_3\text{O}_4/\text{PS}$ composited sponge with Fe_3O_4 -PEI nanoparticles loading content of 10 wt% has been chosen for the following characterizations.

The superhydrophobicity and oleophilicity of MSPS-10%

The surface wettability of the MSPS-10% has been characterized by measuring the water/oil contact angles (W/OCA) on the surface (Fig. 3a). It can be found that the WCA was $155 \pm 0.2^\circ$ and OCA was 0° confirming the surface superhydrophobicity and oleophilicity. To clearly exhibit such wettability, two water droplets (dyed with blue water-based ink) and petroleum ether (dyed with oil red O) were dropped onto the surface of MSPS-10%, in which the water

drops could maintain their spherical shapes, while petroleum ether drops were quickly absorbed. Figure 3b shows the dynamic water adhesion of MSPS-10%. Under an external force, the water droplet contacted the MSPS-10% surface for one minute; however, when the needle tip was moved upward, water droplet left the surface of the material. In addition, when a water droplet fell on the surface of MSPS-10% with a slope of 7° , the water droplet would bounce and rolled on it (Fig. 3c). To prove the uniformity of the whole sponge, three steps were cut within a monolith and the hydrophobicity of each surface has been also measured (Fig. 3d). It could be found that all the water drops (colored by red or blue water-based ink) could maintain their spherical shapes, directly confirming the uniformity of the whole sponge. Given the high porosity, our MSPS-10% also

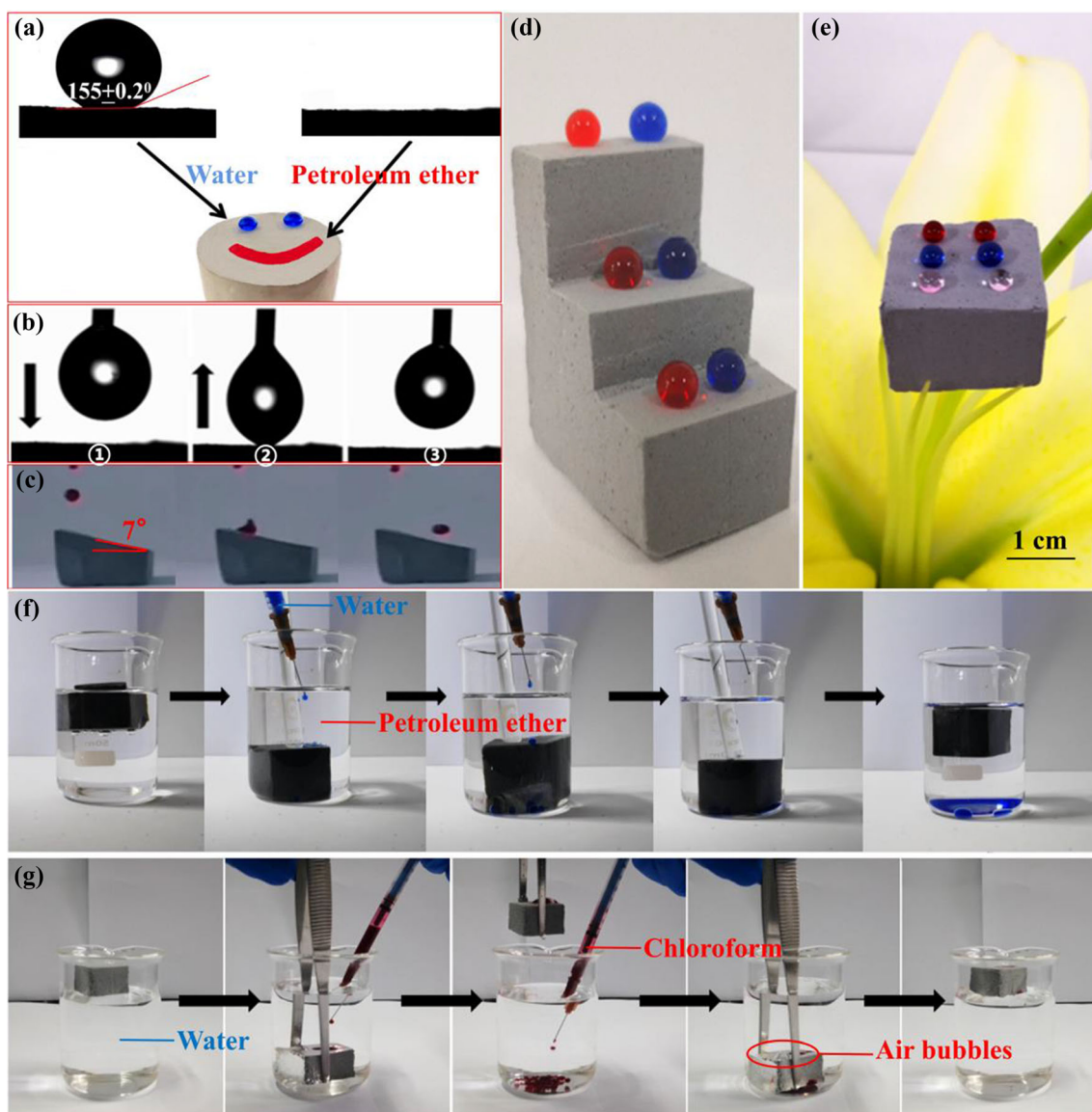


Figure 3 **a** Photograph of water droplets and petroleum ether dropped on MSPS-_{10%}, **b** Dynamic water adhesion of MSPS-_{10%}, **c** The droplet dynamics were captured by high-speed video recording at 500 frames per second, **d** Photograph of water

droplets standing on the steps, **e** MSPS-_{10%} standing on a stamen. **f** Hydrophobic properties of MSPS-_{10%} in petroleum ether, **g** MSPS-_{10%} absorbed chloroform underwater.

displayed ultra-low density (Fig. 3e), which holds great potential for working as high-efficiency oil absorb agent. Figure 3f and Video S1 show that MSPS-_{10%} remains hydrophobic even after oil absorption reached saturation. Organics that cause oil pollution include light oils, as well as heavy oils deposited underwater [46]. When the density of a few oil contaminants is heavier than water, chloroform was concentrated underneath the water. MSPS-_{10%} could be utilized to absorb chloroform underwater; therefore, external forces were used to cause MSPS-

{10%} to contact chloroform. Chloroform was absorbed, and air bubbles were generated on the surface of MSPS-{10%} (Fig. 3g). When there was no oil absorbed in water, air bubbles were not generated on the surface, as shown in Video S2. The reason for this phenomenon is that the interior volume of the MSPS-_{10%} was occupied by chloroform, causing the air stored inside it to be discharged. This phenomenon showed that the surface of MSPS-_{10%} is in a Cassie-Baxter state, which indicated the excellent water repellency of MSPS-_{10%}.

Oil absorption capacity and cycle stability of MSPS-10%

Various organic solvents and oils were used to study the saturated oil absorption capacity of MSPS-10%. In these tests, MSPS-10% was immersed in various organic solvents and oils until it reached oil absorption saturation, and then weighted to give the weight-based absorption capacity (weight (in gram) of solvent or oil absorbed with per gram of MSPS-10%). MSPS-10% displayed different oil absorption capabilities toward various organic solvents and oils. The oil absorption capacity of MSPS-10% toward petroleum ether, toluene, crude oil, acetone and chloroform were 27.8, 35.2, 34.4, 39.4, and 75.3 g/g, respectively (Fig. 4a), which was affected by the viscosity and density of the organic solvents or oils [47]. When the MSPS-10% contacted with organic solvent or oil, the oil penetrates into the material by capillary force. Then, the oil replaces the air volume in the material. Therefore, the greater the density of the oil, the greater the mass of oil absorbed, and the greater the absorption capacity. When MSPS-10% contacted the oil/water mixtures, the organic solvents or oils were drawn into the interior of the porous material due to

capillary forces and low surface energy. Furthermore, on account of the opposite wettability for water and oil, the as-prepared MSPS-10% was utilized to achieve the separation of immiscible oil/water mixtures. Figure 4b shows that the separating device was assembled, which MSPS-10% was cut into round slices and seamlessly fixed in a conical funnel, and then an immiscible oil/water mixture was poured into the funnel. The oil flowed quickly through the MSPS-10% into the beaker, but the water was blocked in the funnel due to the opposite wettability of MSPS-10%. Figure 4a shows that the separation efficiency of MSPS-10% exceeded 99.5% for various immiscible oil–water mixtures. In addition, the absorption capacity and separation efficiency of pristine HPS and the result is shown in Fig. S6. Compared with MSPS-10%, the absorption capacity of HPS increased slightly, may be due to the density of HPS was lower than that of MSPS-10%; the separation efficiency of HPS reduced and due to the hydrophobic performance decreases.

The recycle stability of MSPS-10% is a key factor for its practical oil/water separation applications. Petroleum ether was selected as the target to evaluate the repetitive oil absorption capacity of MSPS-10%. In the cycle tests, MSPS-10% was placed into an oil/water

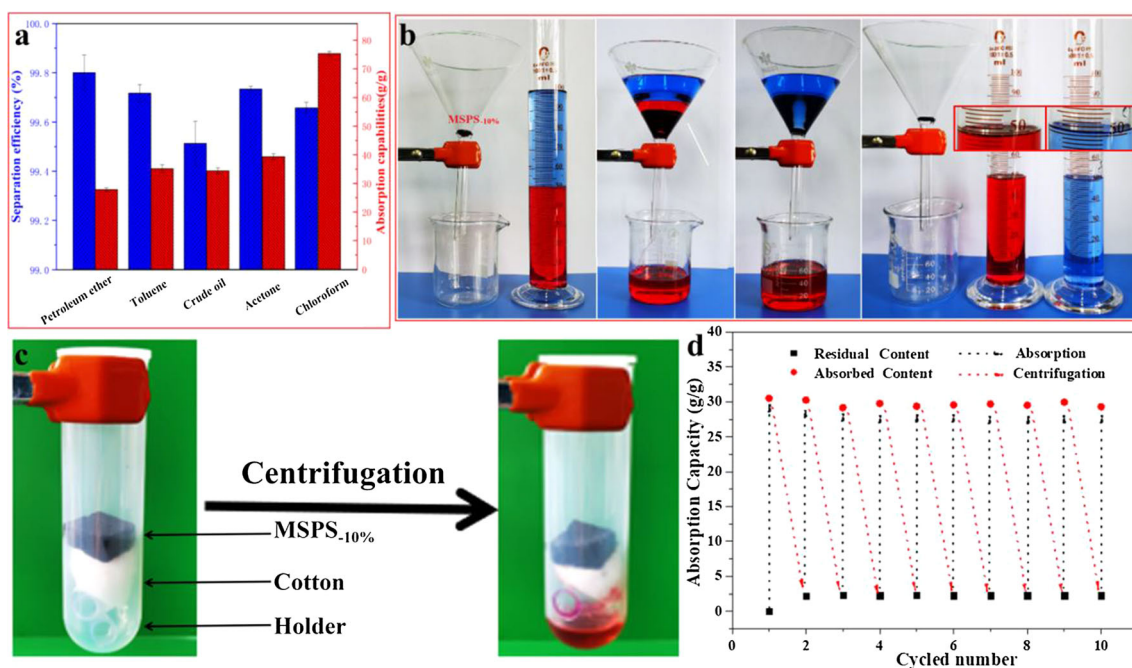


Figure 4 **a** Separation efficiency of MSPS-10% for immiscible oil/water mixtures and the absorption capacity of MSPS-10% for various oils after reaching saturation. **b** Photographs of the oil/water separation process: a piece of MSPS-10% fixed in a conical

funnel to separate a mixture of chloroform (50 mL, dyed with red O) and water (50 mL, dyed with blue water-based ink). **c** Absorption-centrifugation recycling of MSPS-10%. **d** Recycle stability of MSPS-10% for petroleum ether.

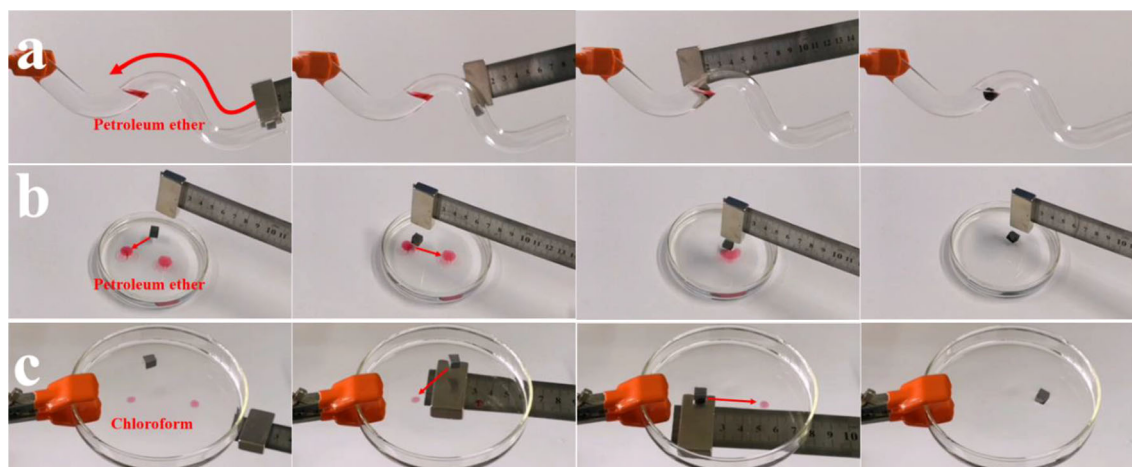


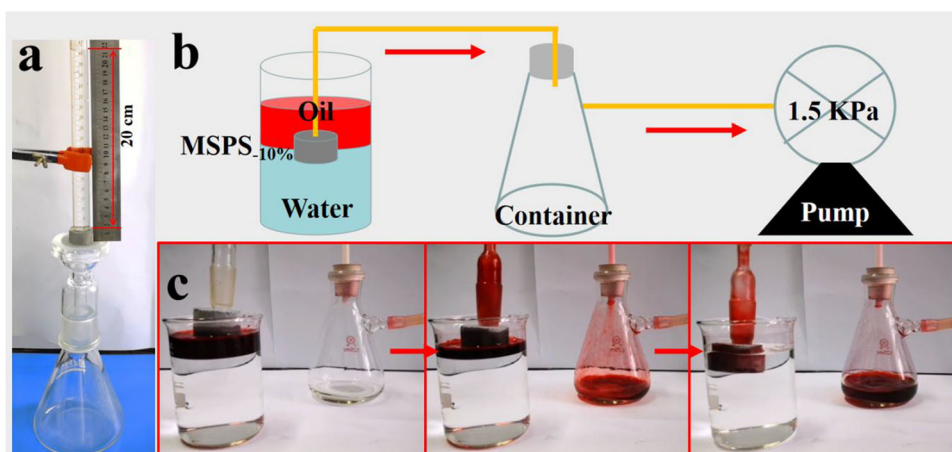
Figure 5 **a** Remote oil removal in confined spaces under magnetic driven. **b** Clean-up of two Petroleum ether droplets from water following pre-designed routes using a magnetically guided MSPS-_{10%}. **c** Cleaning of chloroform from water via magnetic control.

mixture until saturated oil absorption was reached. Then, the grey monolith was removed and weighed. MSPS-_{10%} was then put into a centrifuge tube with a holder and centrifuged at 2000 rpm for 2 min. The grey monolith was weighed to investigate residual oil after centrifugation (Fig. 4c). The regenerated MSPS-_{10%} was used for oil absorption tests in the next cycle. Although the oil absorption performance of MSPS-_{10%} was slightly lower than the original, it still displayed a large oil absorption capacity. The main reason for the slight reduction in its oil absorption was because a small amount (approximately 8%) of petroleum ether in MSPS-_{10%} had not been completely removed by centrifugation (Fig. 4d). This shows that MSPS-_{10%} had stable recycle stability and can be used for practical oil/water separation.

Ability to remove remote oil under magnetic driven

It is necessary to remotely control the removal of oil from oily wastewater under dangerous or severe conditions. When an oil/water mixture existed in a complex and confined pipeline, MSPS-_{10%} was controlled to absorb oil via an external magnetic field (Fig. 5a and Video S3). The sponge was accurately and rapidly guided to the petroleum ether droplets by controlling the direction of the magnetic field. Reaching the oil droplets, the oil was immediately absorbed by the sponge. After cleaning an oil droplet, MSPS-_{10%} was directly guided to the next pollution point for operation (Fig. 5b and Video S4). To prove the precise control and wide applicability of MSPS-_{10%} to absorb oil, MSPS-_{10%} was utilized to clean chloroform according to pre-designed routes (Fig. 5c

Figure 6 **a** The maximum intrusion pressure of water. **b** Schematic of the device for the continuous collection of floating oil. **c** Photographs of the continuous collection of oil.



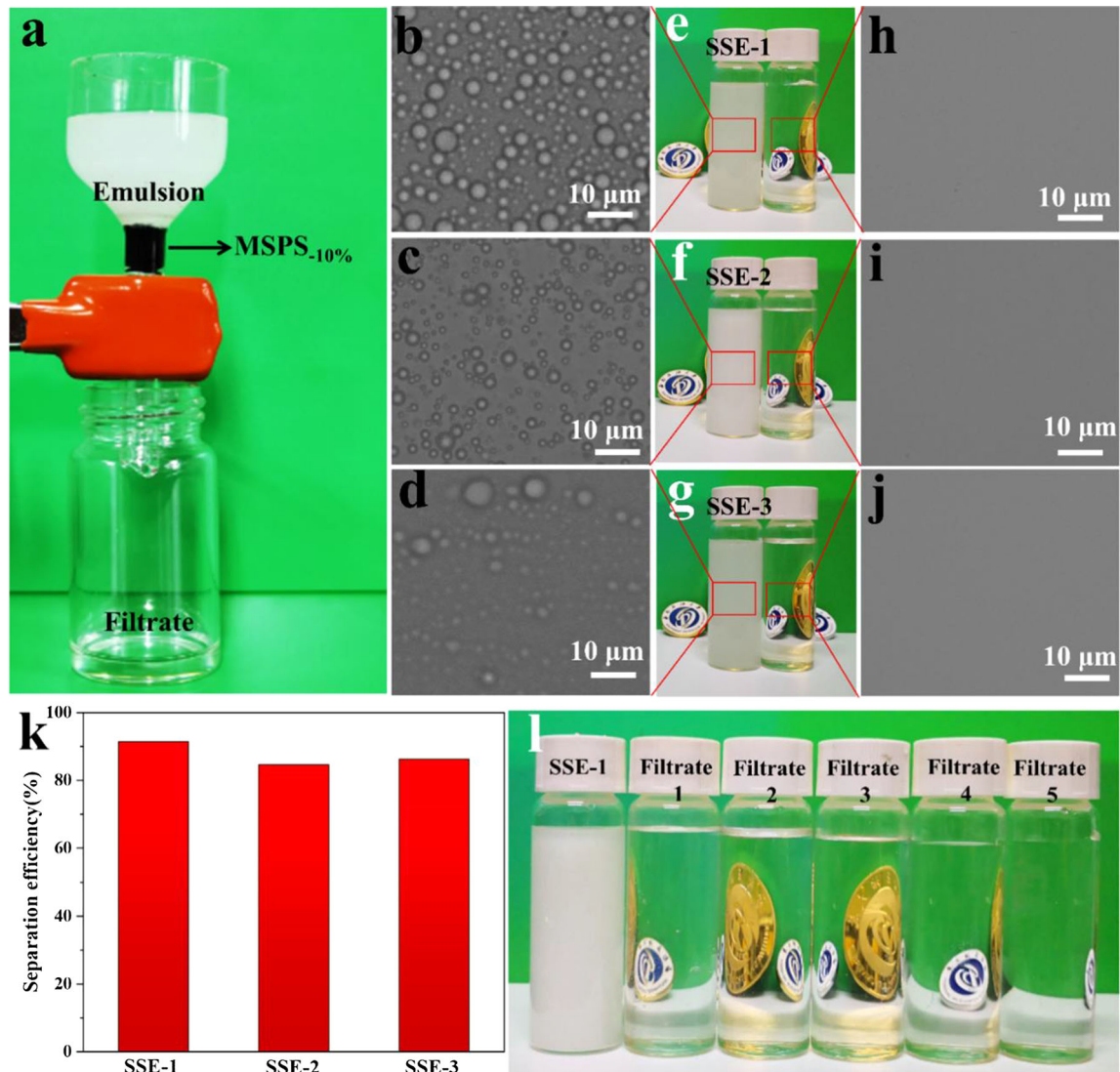


Figure 7 **a** Photograph of Span80-stabilized W/O emulsion separated using MSPS_{-10%}. **b**, **c** and **d** Optical micrograph of Span80-stabilized emulsion. **e**, **f** and **g** Digital photographs of emulsion and filtrate. **h**, **i** and **j** Optical micrograph of filtrate.

and Video S5). Excellent oil absorption capacity and magnetic response characteristics broaden the application range of MSPS_{-10%}.

Continuous oil absorption of MSPS_{-10%}

To be applied for the continuous collection of floating oil, the maximum intrusion pressure of MSPS_{-10%} was investigated. The maximum intrusion pressure was measured by pouring water onto the foam to measure the maximum height (H_{\max}) (Fig. 6a). The intrusion pressure (P) was calculated by the following formula2 [48]:

$$P = \rho g H_{\max}$$

where ρ and g are the density of water and the acceleration of gravity, respectively. The calculated intrusion pressure was about 2 kPa.

According to the method proposed by Ge et al. [49], to continuously collect floating oil in situ from seawater, the dynamic oil/water separation ability of MSPS_{-10%} during pumping was characterized with a simple trapping device. MSPS_{-10%} grey monolith was connected to a tube and placed on the surface of the oil/water mixture, and the other end of this tube was connected to a container with a pump (Fig. 6b). Since

the porous MSPS-10% possesses the opposite wettability for water and oil, during continuous floating oil collection, it quickly absorbed petroleum ether (dyed with oil red O) and blocked water. Eventually, petroleum ether was completely absorbed and transferred into the container (Fig. 6c and Video S6). This continuous floating oil collection device can potentially be used in situ for the emergency treatment of oil spills in offshore oil fields.

Oil/water emulsion separation

Compared with immiscible oil/water mixtures, it is much more difficult to separate oil/water emulsions. In this work, three stable water-in-oil emulsion were prepared with Span80 to simulate the separation oil/water emulsions (Fig. 7a). There were numerous droplets in the milky white water-in-oil emulsion (Fig. 7 b, c, d), but a transparent oil phase was obtained after separation (Fig. 7 e, f and g). An optical microscope image of the collected filtrate in Fig. 7h, i and j showed that no droplets were observed throughout the image. The separation efficiencies of the three surfactant-stabilized water-in-oil emulsions are 92%, 85%, and 86%, respectively (Fig. 7k). In addition, after simple ethanol washing to remove the surfactant attached to the framework, MSPS-10% still has good oil/water emulsion separation performance (Fig. 7l) even after five oil/water emulsion separation/ethanol cleaning cycles [37].

Conclusions

In summary, we have developed a superhydrophobic and magnetic sponge for multi-functional oily wastewater remediation by simply decorating Fe₃O₄ nanoparticles onto a PS sponge substrate. The sponge exhibited a high oil absorption capacity (75 g/g against chloroform) and robust recycling capacity (92% recovery after 10 cycles). The sponge could also be used for continuous oil collection. Interestingly, compared with previous superhydrophobic sponges used for oil/water mixture separation, our sponge could also separate oil/water emulsions by simple filtration under gravity. Given the magnetic properties of Fe₃O₄, oil removal underwater or at some special locations has been also realized. These outstanding functions greatly expand the applications of

superhydrophobic sponges for practical oily wastewater remediation.

Acknowledgements

This research was supported by the Ministry of Science and Technology of China (2019YFE0120300) and the Southwest Petroleum University College Student Open Experiment Key Project (2020KSZ05025).

Declarations

Conflict of interest The authors declare that they have no conflict of interest.

Supplementary Information: The online version contains supplementary material available at <http://doi.org/10.1007/s10853-021-06568-9>.

References

- [1] Almeda R, Wambaugh Z, Wang ZC, Hyatt C, Liu ZF, Buskey EJ (2013) Interactions between zooplankton and crude oil: toxic effects and bioaccumulation of polycyclic aromatic hydrocarbons. *PLoS ONE* 8:212. <https://doi.org/10.1371/journal.pone.0067212>
- [2] Rohal M, Ainsworth C, Lupher B, Montagna PA, Paris CB, Perlin N, Suprenand PM, Yoskowitz D (2020) The effect of the deepwater horizon oil spill on two ecosystem services in the Northern Gulf of Mexico. *Environ Model Softw* 133:104793. <https://doi.org/10.1016/j.envsoft.2020.104793>
- [3] Ainsworth CH, Samhouri JF, Busch DS, Cheung WWL, Dunne J, Okey TA (2011) Potential impacts of climate change on Northeast Pacific marine foodwebs and fisheries. *ICES J Mar Sci* 68:1217–1229. <https://doi.org/10.1093/icesjms/fsr043>
- [4] Ye F, Jiang X, Mi YZ, Kuang JZ, Huang ZM, Yu F, Zhang ZJ, Yuan HK (2019) Preparation of oxidized carbon black grafted with nanoscale silica and its demulsification performance in water-in-oil emulsion. *Colloid Surf A-Physicochem Eng Asp* 582:123878. <https://doi.org/10.1016/j.colsurfa.2019.123878>
- [5] Wang D, Zhao ZQ, Qiao CY, Yang WS, Huang YY, McKay P, Yang DZ, Liu Q, Zeng HB (2020) Techniques for treating slop oil in oil and gas industry: a short review. *Fuel* 279:118482. <https://doi.org/10.1016/j.fuel.2020.118482>
- [6] Aurell J, Gullett BK (2010) Aerostat sampling of PCDD/PCDF emissions from the gulf oil spill in situ burns. *Environ*

- Sci Technol 44:9431–9437. <https://doi.org/10.1021/es103554y>
- [7] Abidli A, Huang YF, Cherukupally P, Bilton AM, Park CB (2020) Novel separator skimmer for oil spill cleanup and oily wastewater treatment: From conceptual system design to the first pilot-scale prototype development. *Environ Technol Innov* 18:100598. <https://doi.org/10.1016/j.eti.2019.100598>
- [8] Su XJ, Li HQ, Lai XJ, Zhang L, Liao XF, Wang J, Chen ZH, He J, Zeng XR (2018) Dual-functional superhydrophobic textiles with asymmetric roll-down/pinned states for water droplet transportation and oil-water separation. *ACS Appl Mater Interfaces* 10:4213–4221. <https://doi.org/10.1021/acami.7b15909>
- [9] Yang RL, Zhu YJ, Chen FF, Qin DD, Xiong ZC (2018) Recyclable, fire-resistant, superhydrophobic, and magnetic paper based on ultralong hydroxyapatite nanowires for continuous oil/water separation and oil collection. *ACS Sustainable Chemistry & Engineering* 6:10140–10150. <https://doi.org/10.1021/acscuschemeng.8b01463>
- [10] Li XP, Cao M, Shan HT, Tezer FH, Li BA (2019) Facile and scalable fabrication of superhydrophobic and superoleophilic PDMS-co-PMHS coating on porous substrates for highly effective oil/water separation. *Chem Eng J* 358:1101–1113. <https://doi.org/10.1016/j.cej.2018.10.097>
- [11] Liu SZ, Zhang Q, Fan LY, Wang R, Yang MJ, Zhou Y (2020) 3D superhydrophobic sponge coated with magnesium hydroxide for effective oil/water mixture and emulsion separation. *Ind Eng Chem Res* 59:11713–11722. <https://doi.org/10.1021/acs.iecr.0c01276>
- [12] Guo HS, Yang J, Xu T, Zhao WQ, Zhang JM, Zhu YN, Wen CY, Li QS, Sui XJ, Zhang L (2019) A robust cotton textile-based material for high-flux oil-water separation. *ACS Appl Mater Interfaces* 11:13704–13713. <https://doi.org/10.1021/acami.9b01108>
- [13] Gu JC, Xiao P, Chen J, Zhang JW, Huang YJ, Chen T (2014) Janus polymer/carbon nanotube hybrid membranes for oil/water separation. *ACS Appl Mater Interfaces* 6:16204–16209. <https://doi.org/10.1021/am504326m>
- [14] Xu Y, Wang G, Zhu L, Shen L, Zhang Z, Ren T, Zeng Z, Chen T, Xue Q (2021) Multifunctional superhydrophobic adsorbents by mixed-dimensional particles assembly for polymorphic and highly efficient oil-water separation. *J Hazard Mater* 407:124374–124374. <https://doi.org/10.1016/j.jhazmat.2020.124374>
- [15] Gao ML, Zhao SY, Chen ZY, Liu L, Han ZB (2019) Superhydrophobic/superoleophilic MOF composites for oil-water separation. *Inorg Chem* 58:2261–2264. <https://doi.org/10.1021/acs.inorgchem.8b03293>
- [16] Lv J, Gong ZJ, He ZK, Yang J, Chen YQ, Tang CY, Liu Y, Fan MK, Lau WM (2017) 3D printing of a mechanically durable superhydrophobic porous membrane for oil-water separation. *Journal of Materials Chemistry A* 5:12435–12444. <https://doi.org/10.1039/c7ta02202f>
- [17] Luo YQ, Song X, Song F, Wang XL, Wang YZ (2019) A fully bio-based composite coating with mechanical robustness and dual superhydrophobicity for efficient two-way oil/water separation. *J Colloid Interface Sci* 549:123–132. <https://doi.org/10.1016/j.jcis.2019.04.055>
- [18] Cao JYQ, Chen SC, Zhang J, Xie YY, Wang YZ (2021) A self-supporting, surface carbonized filter paper membrane for efficient water-in-oil emulsion separation. *Chin J Polym Sci* 39:181–188. <https://doi.org/10.1007/s10118-020-2492-9>
- [19] Li X, Cao M, Shan H, Handan Tezel F, Li B (2019) Facile and scalable fabrication of superhydrophobic and superoleophilic PDMS-co-PMHS coating on porous substrates for highly effective oil/water separation. *Chem Eng J* 358:1101–1113. <https://doi.org/10.1016/j.cej.2018.10.097>
- [20] Zhou S, Hao GZ, Zhou X, Jiang W, Wang TH, Zhang N, Yu LH (2016) One-pot synthesis of robust superhydrophobic, functionalized graphene/polyurethane sponge for effective continuous oil-water separation. *Chem Eng J* 302:155–162. <https://doi.org/10.1016/j.cej.2016.05.051>
- [21] Hou K, Jin Y, Chen JH, Wen XF, Xu SP, Cheng JA, Pi PH (2017) Fabrication of superhydrophobic melamine sponges by thiol-ene click chemistry for oil removal. *Mater Lett* 202:99–102. <https://doi.org/10.1016/j.matlet.2017.05.062>
- [22] Zhang L, Dong DY, Shao LS, Xia YF, Zeng T, Wang YH (2019) Cost-effective one-pot surface modified method to engineer a green superhydrophobic sponge for efficient oil/water mixtures as well as emulsions separation. *Colloid Surf A-Physicochem Eng Asp* 576:43–54. <https://doi.org/10.1016/j.colsurfa.2019.05.022>
- [23] Liu Q, Meng K, Ding K, Wang YB (2015) a superhydrophobic sponge with hierarchical structure as an efficient and recyclable oil absorbent. *ChemPlusChem* 80:1435–1439. <https://doi.org/10.1002/cplu.201500109>
- [24] Zhang JC, Liu X, Chen FZ, Liu JY, Chen Y, Zhang F, Guan NQ (2020) An environmentally friendly and cost-effective method to fabricate superhydrophobic PU sponge for oil/water separation. *J Dispersion Sci Technol* 41:1136–1144. <https://doi.org/10.1080/01932691.2019.1614458>
- [25] Li ZT, He FA, Lin B (2019) Preparation of magnetic superhydrophobic melamine sponge for oil-water separation. *Powder Technol* 345:571–579. <https://doi.org/10.1016/j.powtec.2019.01.035>
- [26] Guselnikova O, Barras A, Addad A, Sviridova E, Szunerits S, Postnikov P, Boukherroub R (2020) Magnetic polyurethane sponge for efficient oil adsorption and separation of oil from oil-in-water emulsions. *Sep Purif Technol* 240:116627. <https://doi.org/10.1016/j.seppur.2020.116627>

- [27] Wu L, Li LX, Li BC, Zhang JP, Wang AQ (2015) Magnetic, durable, and superhydrophobic polyurethane@Fe₃O₄@-SiO₂@fluoropolymer sponges for selective oil absorption and oil/water separation. *ACS Appl Mater Interfaces* 7:4936–4946. <https://doi.org/10.1021/am5091353>
- [28] Li LX, Li BC, Wu L, Zhao X, Zhang JP (2014) Magnetic, superhydrophobic and durable silicone sponges and their applications in removal of organic pollutants from water. *Chem Commun* 50:7831–7833. <https://doi.org/10.1039/c4cc03045a>
- [29] Tran VHT, Lee BK (2017) Novel fabrication of a robust superhydrophobic PU@ZnO@Fe₃O₄@SA sponge and its application in oil-water separations. *Sci Rep* 7:9. <https://doi.org/10.1038/s41598-017-17761-9>
- [30] Liang L, Liu PF, Su HJ, Qian H, Ma HK (2020) One-step fabrication of superhydrophobic sponge with magnetic controllable and flame-retardancy for oil removing and collecting. *J Appl Polym Sci* 137:49353. <https://doi.org/10.1002/app.49353>
- [31] Yu C, Je J, Liu Y, Liu K, Situ Z, Tian L, Luo W, Hong P, Li Y (2020) Facile fabrication of compressible, magnetic and superhydrophobic poly(DVB-MMA) sponge for high-efficiency oil–water separation. *J Mater Sci* 56:3111–3126. <https://doi.org/10.1007/s10853-020-05471-z>
- [32] Ma W, Wang H (2019) Magnetically driven motile superhydrophobic sponges for efficient oil removal. *Appl Mater Today* 15:263–266. <https://doi.org/10.1016/j.apmt.2019.02.004>
- [33] Yu TL, Halouane F, Mathias D, Barras A, Wang ZW, Lv AQ, Lu SX, Xu WG, Meziane D, Tiercelin N, Szunerits S, Boukherroub R (2020) Preparation of magnetic, superhydrophobic/superoleophilic polyurethane sponge: Separation of oil/water mixture and demulsification. *Chem Eng J* 384:1233369. <https://doi.org/10.1016/j.cej.2019.123339>
- [34] He SJ, Zhan YQ, Zhao SM, Lin L, Hu JX, Zhang GY, Zhou M (2019) Design of stable super-hydrophobic/super-oleophilic 3D carbon fiber felt decorated with Fe₃O₄ nanoparticles: facial strategy, magnetic drive and continuous oil/water separation in harsh environments. *Appl Surf Sci* 494:1072–1082. <https://doi.org/10.1016/j.apsusc.2019.07.258>
- [35] Shi Y, Wang B, Ye S, Zhang Y, Wang B, Feng Y, Han W, Liu C, Shen C (2021) Magnetic, superelastic and superhydrophobic porous thermoplastic polyurethane monolith with nano-Fe₃O₄ coating for highly selective and easy-recycling oil/water separation. *Appl Surf Sci* 535:147690. <https://doi.org/10.1016/j.apsusc.2020.147690>
- [36] Li JN, Wang FJ, Wan H, Liu J, Liu ZY, Cheng K, Zou HF (2015) Magnetic nanoparticles coated with maltose-functionalized polyethyleneimine for highly efficient enrichment of N-glycopeptides. *J Chromatogr A* 1425:213–220. <https://doi.org/10.1016/j.chroma.2015.11.044>
- [37] Yang J, Wang H, Tao Z, Liu X, Wang Z, Yue R, Cui Z (2019) 3D superhydrophobic sponge with a novel compression strategy for effective water-in-oil emulsion separation and its separation mechanism. *Chem Eng J* 359:149–158. <https://doi.org/10.1016/j.cej.2018.11.125>
- [38] Zhang H, Zhong X, Xu JJ, Chen HY (2008) Fe₃O₄/Polypyrrole/Au nanocomposites with core/shell/shell structure: synthesis, characterization, and their electrochemical properties. *Langmuir* 24:13748–13752. <https://doi.org/10.1021/la8028935>
- [39] Wang YF, Xu F, Zhang L, Wei XL (2013) One-pot solvothermal synthesis of Fe₃O₄-PEI composite and its further modification with Au nanoparticles. *J Nanopart Res* 15:107. <https://doi.org/10.1007/s11051-012-1338-y>
- [40] Pulko I, Krajnc P (2012) High internal phase emulsion templating - a path to hierarchically porous functional polymers. *Macromol Rapid Commun* 33:1731–1746. <https://doi.org/10.1002/marc.201200393>
- [41] Wang ZY, Stein A (2008) Morphology control of carbon, silica, and carbon/silica nanocomposites: from 3D ordered Macro-/Mesoporous monoliths to shaped mesoporous particles. *Chem Mater* 20:1029–1040. <https://doi.org/10.1021/cm0717864>
- [42] Zhang N, Zhong S, Zhou X, Jiang W, Wang T, Fu J (2016) Superhydrophobic P (St-DVB) foam prepared by the high internal phase emulsion technique for oil spill recovery. *Chem Eng J* 298:117–124. <https://doi.org/10.1016/j.cej.2016.03.151>
- [43] Foudazi R (2021) HIPEs to PolyHIPEs. *React Funct Polym* 164:104917. <https://doi.org/10.1016/j.reactfunctpolym.2021.104917>
- [44] Xu L, Chen Y, Liu N, Zhang W, Yang Y, Cao Y, Lin X, Wei Y, Feng L (2015) Breathing demulsification: a three-dimensional (3D) free-standing superhydrophilic sponge. *ACS Appl Mater Interfaces* 7:22264–22271. <https://doi.org/10.1021/acsami.5b07530>
- [45] Paljevack M, Krajnc P (2020) Hierarchically porous poly(glycidyl methacrylate) through hard sphere and high internal phase emulsion templating. *Polymer* 209:123064. <https://doi.org/10.1016/j.polymer.2020.123064>
- [46] Cao GL, Zhang WB, Jia Z, Liu F, Yang HY, Yu QQ, Wang YZ, Di X, Wang CY, Ho SH (2017) Dually prewetted underwater superoleophobic and under oil superhydrophobic fabric for successive separation of light oil/water/heavy oil three-phase mixtures. *ACS Appl Mater Interfaces* 9:36368–36376. <https://doi.org/10.1021/acsami.7b08997>
- [47] Zhang WB, Shi Z, Zhang F, Liu X, Jin J, Jiang L (2013) Superhydrophobic and superoleophilic PVDF membranes

- for effective separation of water-in-oil emulsions with high flux. *Adv Mater* 25:2071–2076. <https://doi.org/10.1002/adma.201204520>
- [48] Zhou WT, Li S, Liu Y, Xu ZZ, Wei SF, Wang GY, Lian JS, Jiang Q (2018) Dual superlyophobic copper foam with good durability and recyclability for high flux, high efficiency, and continuous oil-water separation. *ACS Appl Mater Interfaces* 10:9841–9848. <https://doi.org/10.1021/acsami.7b19853>
- [49] Ge J, Ye YD, Yao HB, Zhu X, Wang X, Wu L, Wang JL, Ding H, Yong N, He LH, Yu SH (2014) Pumping through porous hydrophobic/oleophilic materials: an alternative technology for oil spill remediation. *Angew Chem-Int Edit* 53:3612–3616. <https://doi.org/10.1002/anie.201310151>

Publisher's Note Springer Nature remains neutral with regard to jurisdictional claims in published maps and institutional affiliations.